www.sciencemag.org/cgi/content/full/338/6111/1220/DC1

Supplementary Materials for

Progenitor and Terminal Subsets of CD8$^+$ T Cells Cooperate to Contain Chronic Viral Infection

Michael A. Paley, Daniela C. Kroy, Pamela M. Odorizzi, Jonathan B. Johnnidis, Douglas V. Dolfi, Burton E. Barnett, Elizabeth K. Bikoff, Elizabeth J. Robertson, Georg M. Lauer, Steven L. Reiner, E. John Wherry*

*To whom correspondence should be addressed. E-mail: wherry@mail.med.upenn.edu

Published 30 November 2012, *Science* **338**, 1220 (2012)
DOI: 10.1126/science.1229620

This PDF file includes:

Supplementary Materials:

Materials and Methods:

Human Subjects:

All human subjects were recruited at the Massachusetts General Hospital Gastrointestinal Unit and the Department of Surgery in accordance with the IRB approved study: "Cell mediated immunity in Hepatitis C virus infection"; Protocol # 1999-P-004983/54; MGH Legacy #: 90-7246. Liver specimens were obtained from explantation or resection of 8 patients with at least 5 years of chronic HCV infection, defined by positive anti-HCV antibody and detectable viral load. Three patients with treatment induced sustained virological response (SVR, undetectable viral load 6 months after end of treatment) were analyzed. SVR of all 3 patients was achieved at least 3 years prior to liver sampling. Intrahepatic lymphocytes (IHL) were extracted by mechanical disruption of liver tissue. The cell suspension was then washed twice in RPMI 1640 culture medium supplemented with 10% FBS, followed by centrifugation at 300 rpm each time to remove cell debris and hepatocytes. The final washing step was followed by centrifugation at 1500 rpm to obtain a pellet of IHL.

Mice and Infections:

All animals were housed at the University of Pennsylvania (Philadelphia, PA). Experiments were performed in accordance with protocols approved by the University of Pennsylvania Institutional Animal Care and Use Committee. $Eomes^{flox/flox}$, $Eomes^{gfp/+}$, and $Tbx21^{-/-}$ (T-bet KO) mice have been described previously (*7, 20, 32*). To examine $CD8^{+}$ T cell differentiation in the absence of Eomes, $Eomes^{flox/flox}$ mice were crossed to

CD4-Cre mice (Eomes cKO) (*7*). CD4-Cre^{+} Eomes$^{+/+}$ or littermate CD4-Cre^{-} Eomes$^{f/f}$ mice were used as WT controls. Mice were infected with either 2 x 10^5 PFU of lymphocytic choriomenigitis virus (LCMV) Armstrong strain by i.p. injection to generate an acutely resolved infection or 4 x 10^6 PFU of LCMV clone 13 strain by i.v. injection to generate a chronic infection. The V35A variant of clone 13 has been previously described (*19, 33*).

Flow cytometry and real-time PCR:

All cells were stained with LIVE/DEAD® Fixable Dead Cell Stain (Invitrogen) to discriminate live from dead cells. Surface staining was performed as described previously (*7, 34*). Intracellular staining was performed using the Foxp3 / Transcription Factor Staining Buffer Set per manufacturer's instructions (eBioscience; San Diego, CA). Antibodies used for flow cytometry were purchased from BD Biosciences (CD4, CD8, CD19, CD44, 2B4, Ki-67; San Jose, CA), Biolegend (PD-1, Tim3, TNF-α, IFN-γ, T-bet; San Diego, CA), R&D Systems (MIP-1α; Minneapolis, MN), or eBioscience (CD8, Lag3, CD160, 2B4, CD45.1, CD45.2, CD107a, Eomes). MHC class I peptide tetramers were made and used as described previously (*30, 35*). Data were collected on a BD LSRII (BD Biosciences) and analyzed with FlowJo software (Tree Star, Ashland, OR). Cell sorting was performed using a BD Aria II (BD Biosciences). qRT-PCR was carried out as previously described (*7, 36*). Gene expression was normalized to GAPDH. Target gene probes were purchased from Applied Biosystems (Foster City, CA).

Total Body Estimation of Blood, Skin, and Bone Marrow:

Mice were weighed for total blood volume and surface area estimation. Total blood volume was estimated as 6% body weight (*37*). Total skin surface area (in cm^2) was estimated as 9.822 * (mass in g)$^{0.667}$ as described in (*38*). Total body bone marrow was estimated to be 7.9-fold of the yield from two femurs as previously described (*35, 39, 40*). Tissues were processed and hematopoietic cells isolated as described (*35*).

Bone Marrow Chimeras

Bone marrow (BM) from WT (CD45.1$^+$), T-bet KO (CD45.2$^+$), and Eomes cKO (CD45.2$^+$) donors was harvested. 5-10 x 10^6 donor cells were transferred i.v. into sublethally irradiated (450 rads) *Rag2*$^{-/-}$ recipients. 8 weeks after BM transfer, chimeras were infected with LCMV clone 13.

BrdU Treatment and Detection

Animals were treated with 2mg of BrdU (Sigma-Aldrich; St. Louis, MO) i.p. daily for 7 days prior to tissue harvest and analysis. BrdU incorporation was assessed by the BrdU Flow Kit per manufacturer's instructions (BD Biosciences).

CFSE labeling, temporal deletion and adoptive transfers:

At indicated days p.i., spleens were harvested from indicated CD45.2$^+$ donor mice. CD8$^+$ T cells were purified from splenocytes using magnetic beads according to manufacturer's protocol (CD8 negative selection; MACS beads; Miltenyi Biotec, Auburn, CA). Purified CD8$^+$ T cells were labeled with CFSE as described previously (*30, 35*),

and transferred i.v. into CD45.1$^+$ infection-matched controls. Temporal Eomes deletion with Tat-Cre was performed as described (*36*).

Statistical Analysis:

Student's t test (Paired and Unpaired), Mann-Whitney test, and 2-way ANOVA were performed using Prism software (Graphpad, La Jolla, CA).

Figure Legends

Figure S1. Eomes expression is enhanced during chronic viral infection and segregates antiviral CD8$^+$ T cells with distinct functional properties. (A) Flow cytometric analysis of GFP expression in D^{b}gp33-specific CD8$^+$ T cells in WT (shaded) or *Eomes$^{gfp/+}$* (open) mice at indicated days p.i. (B) Flow cytometric analysis of YFP (Blimp1) versus GFP (Eomes) expression in D^{b}gp33-specific CD8$^+$ T cells on d8 post LCMV Armstrong infection of WT, single, or double reporter mice as indicated. (C) Flow cytometric analysis of IFN-γ and TNF-α expression in Eomes^{hi} and Eomes^{lo} virus-specific CD8$^+$ T cells after stimulation with indicated LCMV peptides on d22 p.i. (2-way ANOVA). (D) Flow cytometric analysis of granzyme B expression in naïve (shaded) or Eomes$^+$ and Eomes$^-$ D^{b}gp276-specifc CD8$^+$ T cells (open) d22 post clone 13 infection. (A-D) Numbers denote frequency of gated population. (A-D) Data are representative of 2-5 independent experiments with at least three mice per experimental group. (E) Flow cytometric analysis of CD107a staining of naïve (shaded) or Eomes$^+$ and Eomes$^-$ MIP-1α^+ CD8$^+$ T cells (open) after stimulation with gp276-286 peptide on d23 p.i. post clone 13 infection. Data is aggregated across three independent experiments. (F) PD-1

expression effectively separates cells with elevated T-bet (T-bet^{hi}) versus elevated Eomes (Eomes^{hi}). Flow cytometric analysis of T-bet, Eomes, and PD-1 expression in D^{b}gp33-specific CD8^{+} T cells d21 post clone 13 infection. (G) Eomes^{hi} cells have enhanced cytotoxicity compared to T-bet^{hi} cells. Cytotoxicity of sorted PD-1^{int} (T-bet^{hi}) and PD-1^{hi} (Eomes^{hi}) D^{b}gp33-specific CD8^{+} T cells on d22 p.i. (H) 2,000 *Eomes$^{gfp/+}$* TCR-transgenic D^{b}gp33-specific (P14) CD8^{+} T cells were transferred into naïve recipients one day before infection with clone 13. Donor P14 cells from chronically infected mice were isolated on d22 p.i., sorted based on GFP expression, and added to target cells pulsed with LCMV-derived peptide gp33-41. % specific lysis was determined by the loss of target cells compared to control cells. Graphs display mean ± S.E.M. (D, E, H) (*p<0.05, **p<0.01; Paired t test). (F-H) Data are representative of 2-5 independent experiments.

Figure S2. Genetic deletion of Eomes leads to loss of the T-bet^{lo} PD-1^{hi} population of exhausted CD8^{+} T cells. Rag KO hosts were sublethally irradiated and reconstituted with a 1:1 mixture of WT and EKO bone marrow, followed by infection with LCMV clone 13. (A) Flow cytometric analysis of T-bet and PD-1 expression in D^{b}gp276-specific CD8^{+} T cells d60 p.i. Numbers denote frequency of gated population. (B) MFI of T-bet and PD-1 expression from cells in (A). (*p<0.05, **p<0.01; Paired t test). All data are representative of 3 independent experiments with at least four mice.

Figure S3. T-bet^{hi} and Eomes^{hi} exhausted CD8^{+} T cell subsets have distinct population size and anatomical distribution. (A) Eomes^{hi} cells outnumber T-bet^{hi}

cells. T-bet^{hi} and Eomes^{hi} populations of D^{b}gp276-specific CD8^{+} T cells were quantified for the total mouse (see Methods). Graph displays sum of all tissues in (B). (B) Individual organs contain distinct proportions of T-bet^{hi} and Eomes^{hi} populations. The frequency of T-bet^{hi} and Eomes^{hi} populations of D^{b}gp276-specific CD8^{+} T cells are displayed for each indicated organ. (C) Quantification of T-bet^{hi} and Eomes^{hi} populations of D^{b}gp276-specific CD8^{+} T cells are displayed for each indicated organ. (D) CD8^{+} T cells from chronically infected CD45.2 mice were isolated d22 p.i. post clone 13 infection, sorted based on PD-1 expression and adoptively transferred into infection-matched CD45.1 recipient mice. (E) Two weeks post-transfer, virus-specific CD8^{+} T cells were enumerated in indicated organs. All graphs display mean ± S.E.M. (*$p<0.05$; Unpaired t test). All data are representative of 2-5 independent experiments with at least three mice per experimental group.

Figure S4. T-bet and Eomes-dependent populations exhibit differential proliferation. (A) Flow cytometric analysis of T-bet, Eomes, and PD-1 versus Ki-67 expression in D^{b}gp33-specific CD8^{+} T cells on d22 p.i. (B) Representative gating strategy for T-bet^{hi} and T-bet^{lo} populations for **Fig 2A, 2B.** (C) Flow cytometric analysis of Eomes expression versus BrdU incorporation for D^{b}gp276-specific CD8^{+} T cells in indicated tissues. (A-C) Data are representative of 3-4 independent experiments with at least three mice per experimental group. (D) CD8^{+} T cells from CD45.2 LCMV clone 13 chronically infected mice were isolated d15 p.i., CFSE-labeled, and transferred into clone 13 infection-matched CD45.1 recipient mice. One week post-transfer, virus-specific CD8^{+} T cells were analyzed for CFSE dilution. (E) CD8^{+} T cells from CD45.2

LCMV Armstrong-immune (d30+) or clone 13 chronically infected (d30) mice were isolated, CFSE-labeled, and transferred into LCMV Armstrong-immune (d30+) or chronically infected (d30) CD45.1 recipient mice. One week post-transfer, virus-specific $CD8^+$ T cells were analyzed for CFSE dilution. (F) Flow cytometric analysis of CFSE dilution in D^bgp33-specific donor $CD8^+$ T cells. Data are representative of 2 independent experiments. (G) Flow cytometric analysis of Ki-67 expression in D^bgp33-specific $CD8^+$ T cells from WT, T-bet KO, and Eomes cKO mice at indicated days p.i. (***$p<0.001$; Unpaired t test). Data are aggregated across 2 independent experiments.

Figure S5. T-bet^{hi} Eomes^{lo} CD8$^+$ T cells convert to T-bet^{lo} Eomes^{hi} CD8$^+$ T cells. (A) $CD8^+$ T cells from chronically infected CD45.2 mice were isolated d22 p.i. with LCMV clone 13, sorted based on PD-1 expression, CFSE-labeled, and transferred into infection-matched CD45.1 recipient mice. One week post-transfer, virus-specific $CD8^+$ T cells were analyzed for CFSE dilution. (B) Flow cytometric analysis of PD-1 expression versus CFSE dilution of sorted donor D^bgp276$^+$$CD8^+$ T cells in indicated organs. Populations in division 0-2, 3-6, and 7+ are indicated. Quantification of the indicated division is provided from the liver. Graph displays mean ± S.E.M. (*$p<0.05$; Unpaired t test) (C) $CD8^+$ T cells from chronically infected *Eomes*$^{gfp/+}$ mice were isolated d15 p.i. with clone 13, sorted based on GFP expression, and adoptively transferred into infection-matched CD45.1 recipient mice. Two weeks post-transfer, virus-specific $CD8^+$ T cells were analyzed for GFP expression. (D) Flow cytometric analysis of GFP expression (open) of sorted D^bgp276-specific *Eomes*$^{gfp/+}$ $CD8^+$ T cells 2 weeks post-transfer. (D) $CD8^+$ T cells from chronically infected *Eomes*$^{+/+}$ or *Eomes*$^{f/f}$ mice were

isolated d15 p.i. with clone 13, treated with Tat-Cre *in vitro*, CFSE-labeled, and adoptively transferred into infection-matched CD45.1 recipient mice. Two weeks post-transfer, virus-specific $CD8^+$ T cells were analyzed for CFSE dilution. (E) $CD8^+$ T cells from chronically infected *T-bet*$^{+/+}$ or *T-bet*$^{f/f}$ mice were isolated d15 p.i. with clone 13, treated with Tat-Cre *in vitro*, CFSE-labeled, and adoptively transferred into infection-matched CD45.1 recipient mice. Two weeks post-transfer, virus-specific $CD8^+$ T cells were analyzed for CFSE dilution. (B, D) All data are representative of 3-4 independent experiments with 1-3 mice per experimental group.

Figure S6. Loss of either T-bet or Eomes leads to reduced $CD8^+$ T cell responses during chronic infection. Quantification of D^bgp276-specific $CD8^+$ T cells from indicated organs of WT, T-bet KO (TKO), and EKO mice at d30 p.i. (*p<0.05, **p<0.01, ***p<0.001; Paired t test). Data are representative of 2 independent experiments with at least three mice per experimental group.

Figure S7. Eomes acts cell-intrinsically to maintain $CD8^+$ T cell responses. Mixed bone-marrow chimeras were generated as in Fig. S2. (A) Longitudinal frequency of D^bgp33-specific $CD8^+$ T cells in the blood of infected mice. (B) Total D^bgp33-specific and D^bgp276-specific $CD8^+$ T cells in the spleens infected mice d60 p.i. (*p<0.05; Paired t test). All data are representative of 3 independent experiments with at least four mice group.

Figure S8. Deletion of Eomes leads to impaired viral control. WT, TKO, and EKO mice were infected with LCMV clone 13 and assessed for viral control. Graphs display viral load in indicated tissues d90 p.i. Data are representative of 2 independent experiments with at least three mice per experimental group.

Figure S9. Loss of Eomes^{hi} progeny after removal of antigen is due to poor repopulation from T-bet^{hi} progenitors. (A) CD8^{+} T cells from chronically infected CD45.2 mice were isolated d22 p.i., sorted based on PD-1 expression, and CFSE-labeled. Equal numbers of D^{b}gp33-specific CD8^{+} T cells were adoptively transferred into WT or V35A infection-matched CD45.1 recipient mice. Two weeks post-transfer, virus-specific CD8^{+} T cells were analyzed for CFSE dilution. (B) 2,000 *Eomes$^{gfp/+}$* TCR-transgenic D^{b}gp33-specific (P14) CD8^{+} T cells were adoptively transferred into naïve recipients one day before infection with clone 13. Donor P14 cells from chronically infected mice were isolated d22 p.i., sorted based on GFP expression, and adoptively transferred into WT or V35A infection-matched recipient mice. Two weeks post-transfer, donor P14 CD8^{+} T cells were analyzed for GFP expression. (C) Flow cytometric analysis and quantification of GFP expression in sorted donor P14 CD8^{+} T cells. Graph displays mean ± S.E.M. (*$p<0.05$; Unpaired t test). Data are representative three mice per experimental group.

Figure S10. Continued preferential BrdU incorporation in Eomes^{hi} cells after months of sustained viremia. Flow cytometric analysis of Eomes and PD-1 expression versus BrdU incorporation in D^{b}gp276-specific CD8^{+} T cells from CD4

depleted WT mice at d250 p.i. with clone 13. All data are representative of four mice across 2 independent experiments.

Figure S11. T-bet and Eomes expression in systemic anti-HCV responses.

Frequency of Eomes^{hi} and T-bet^{hi} HCV-specific CD8^{+} T cells from the blood of subjects with resolved or chronic infection. ($p > 0.05$; Unpaired t test).

Figure S1

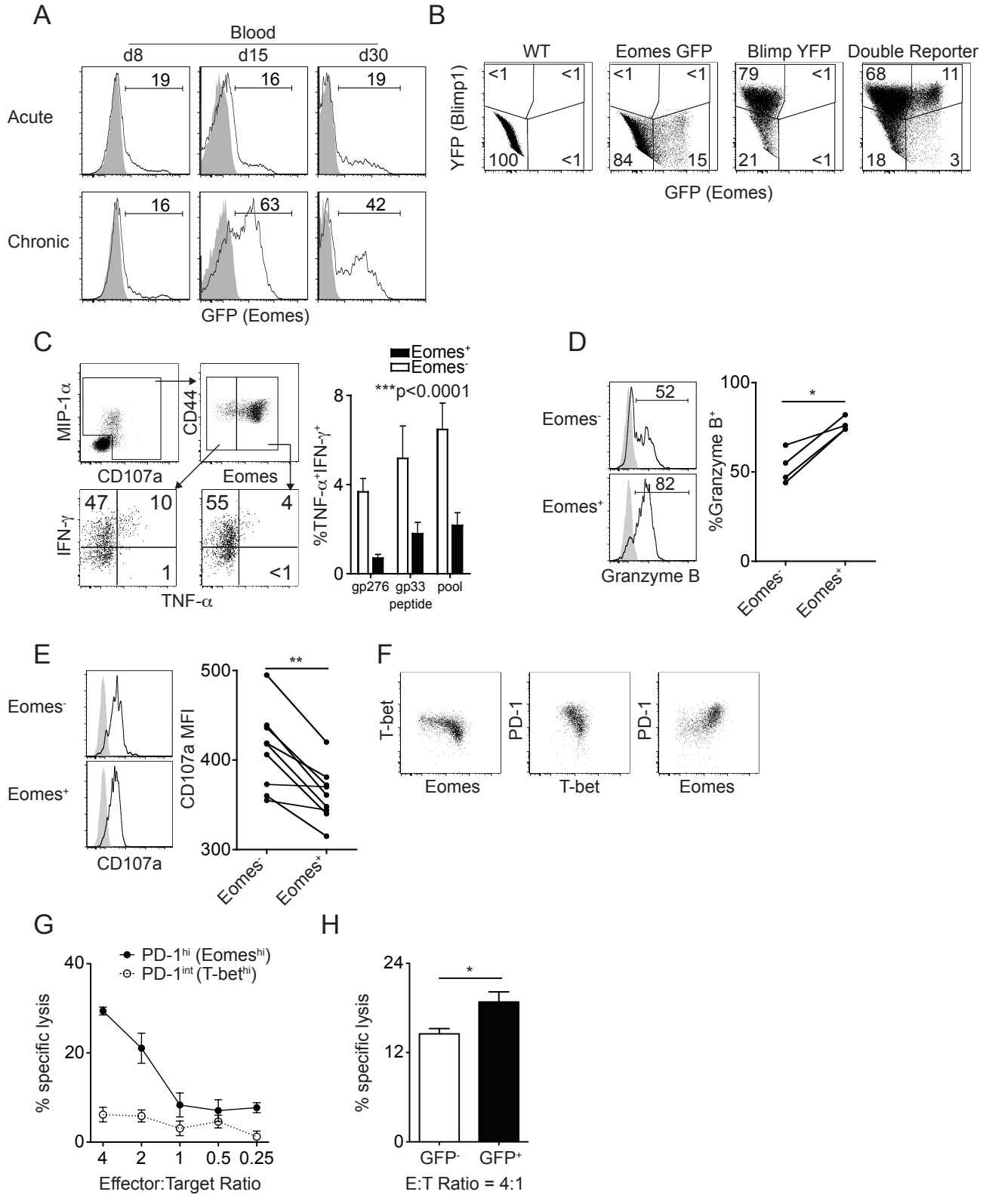
A
Blood
d8
d15
d30
Acute
Chronic
19
16
19
16
63
42
GFP (Eomes)
B
WT
Eomes GFP
Blimp YFP
Double Reporter
YFP (Blimp1)
GFP (Eomes)
C
MIP-1α
CD44
CD107a
Eomes
IFN-γ
TNF-α
47
10
1
55
4
<1
Eomes+
Eomes-
***p<0.0001
%TNF-α+IFN-γ+
gp276
gp33
pool
peptide
D
Eomes-
Eomes+
52
82
Granzyme B
%Granzyme B+
*
E
Eomes-
Eomes+
CD107a
CD107a MFI
**
F
T-bet
Eomes
PD-1
T-bet
PD-1
Eomes
G
PD-1hi (Eomeshi)
PD-1int (T-bethi)
% specific lysis
Effector:Target Ratio
H
% specific lysis
GFP-
GFP+
E:T Ratio = 4:1
*

Figure S2

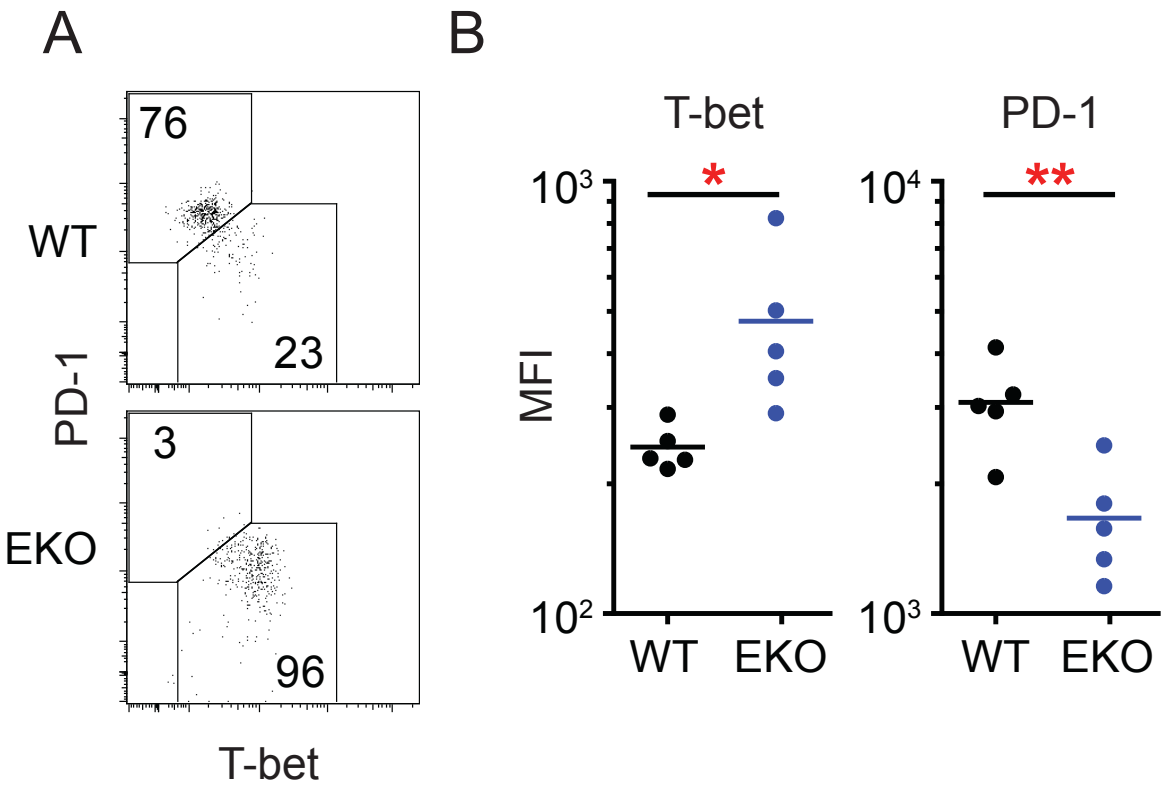
A
B
76
23
3
96
WT
EKO
PD-1
T-bet
T-bet
PD-1
MFI
10^3
10^2
10^4
10^3
*
**
WT
EKO
WT
EKO

Figure S3

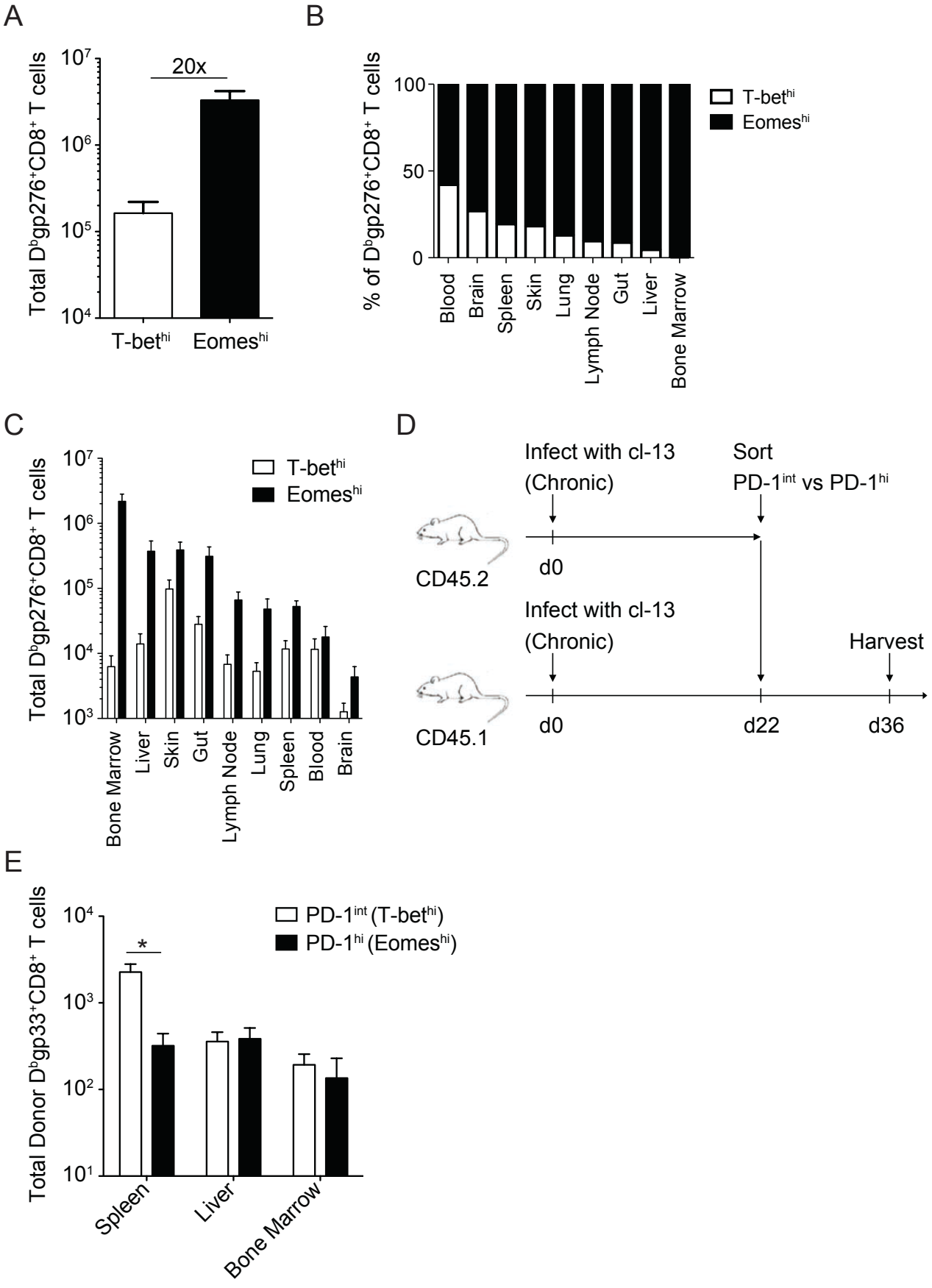
A
B
C
D
E
20x
Total Dbgp276+CD8+ T cells
T-bethi
Eomeshi
% of Dbgp276+CD8+ T cells
Blood
Brain
Spleen
Skin
Lung
Lymph Node
Gut
Liver
Bone Marrow
Infect with cl-13
(Chronic)
Sort
PD-1int vs PD-1hi
CD45.2
d0
Infect with cl-13
(Chronic)
Harvest
CD45.1
d0
d22
d36
Total Donor Dbgp33+CD8+ T cells
PD-1int (T-bethi)
PD-1hi (Eomeshi)
*
Spleen
Liver
Bone Marrow

Figure S4

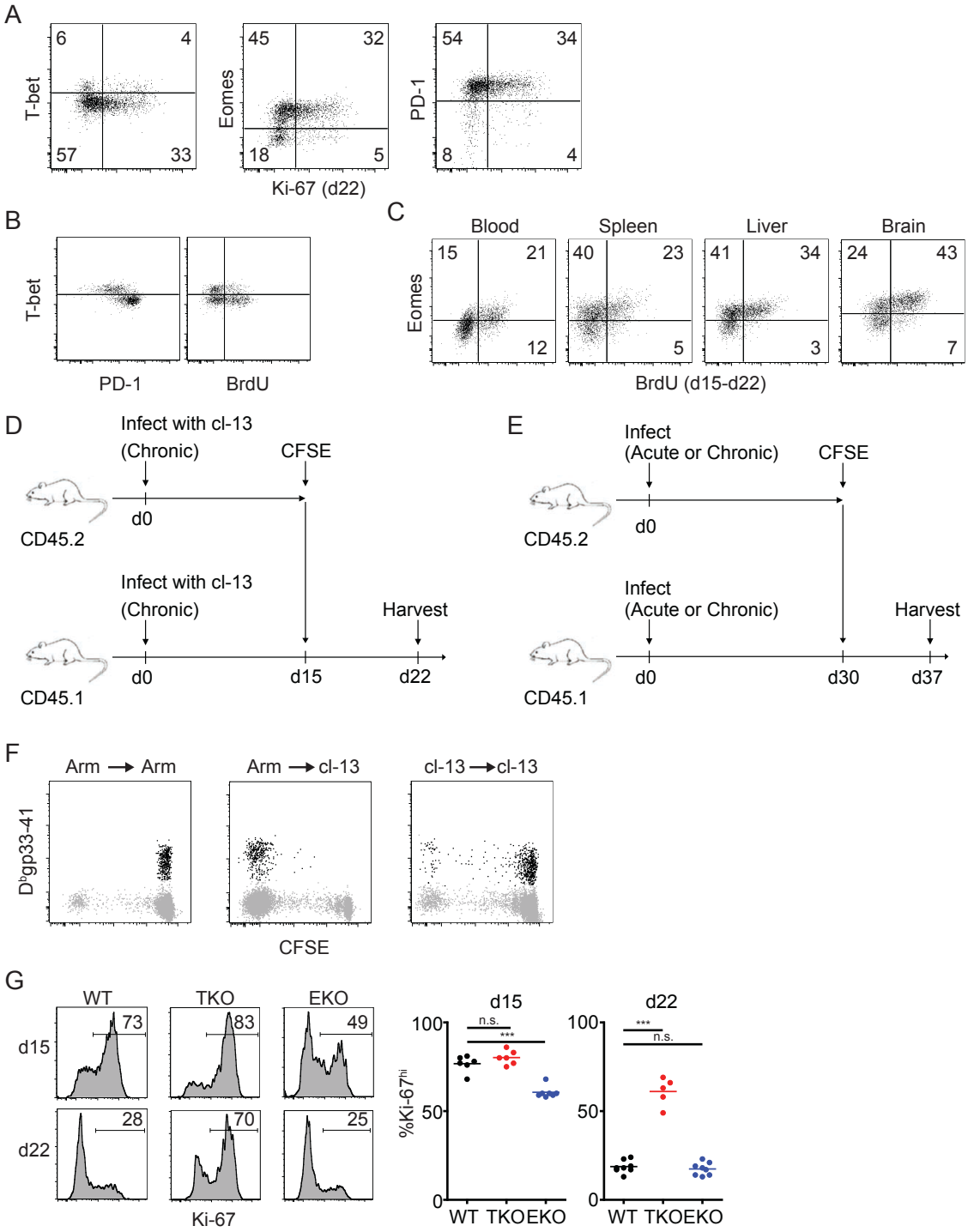
A
T-bet
Eomes
Ki-67 (d22)
PD-1
B
T-bet
PD-1
BrdU
C
Blood
Spleen
Liver
Brain
Eomes
BrdU (d15-d22)
D
Infect with cl-13
(Chronic)
CFSE
CD45.2
d0
Infect with cl-13
(Chronic)
Harvest
CD45.1
d0
d15
d22
E
Infect
(Acute or Chronic)
CFSE
CD45.2
d0
Infect
(Acute or Chronic)
Harvest
CD45.1
d0
d30
d37
F
Arm → Arm
Arm → cl-13
cl-13 → cl-13
DbGP33-41
CFSE
G
WT
TKO
EKO
d15
d22
Ki-67
d15
d22
%Ki-67hi
n.s.
***
WT TKO EKO

Figure S5

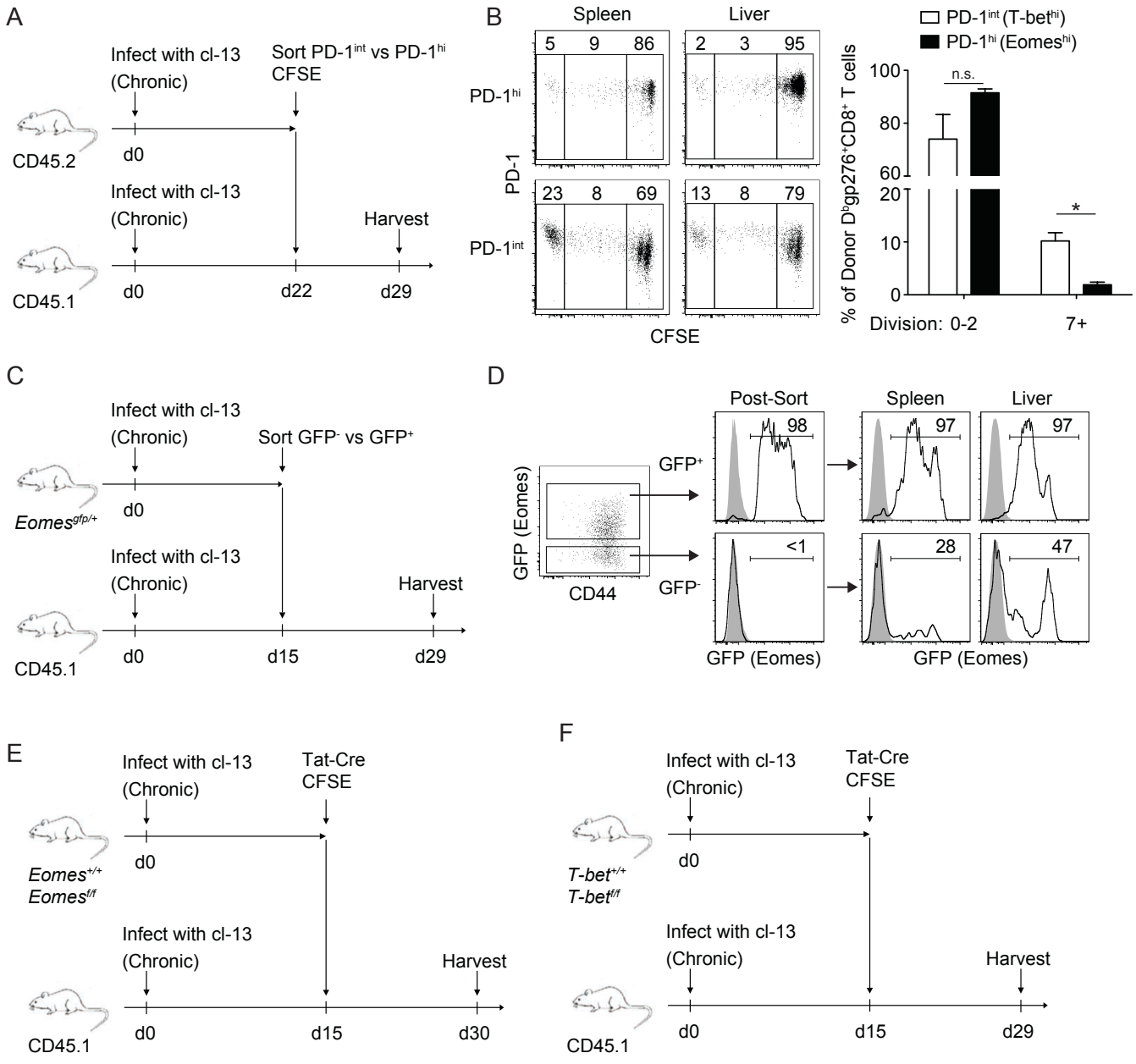
A
Infect with cl-13
(Chronic)
Sort PD-1int vs PD-1hi
CFSE
CD45.2
d0
Infect with cl-13
(Chronic)
Harvest
CD45.1
d0
d22
d29
B
Spleen
Liver
5 9 86
2 3 95
PD-1hi
PD-1
23 8 69
13 8 79
PD-1int
CFSE
PD-1int (T-bethi)
PD-1hi (Eomeshi)
% of Donor Dbgp276+CD8+ T cells
100
80
60
20
10
0
n.s.
*
Division: 0-2
7+
C
Infect with cl-13
(Chronic)
Sort GFP- vs GFP+
Eomesgfp/+
d0
Infect with cl-13
(Chronic)
Harvest
CD45.1
d0
d15
d29
D
Post-Sort
Spleen
Liver
GFP (Eomes)
CD44
GFP+
GFP-
98
97
97
<1
28
47
GFP (Eomes)
GFP (Eomes)
E
Infect with cl-13
(Chronic)
Tat-Cre
CFSE
Eomes+/+
Eomesf/f
d0
Infect with cl-13
(Chronic)
Harvest
CD45.1
d0
d15
d30
F
Infect with cl-13
(Chronic)
Tat-Cre
CFSE
T-bet+/+
T-betf/f
d0
Infect with cl-13
(Chronic)
Harvest
CD45.1
d0
d15
d29

Figure S6

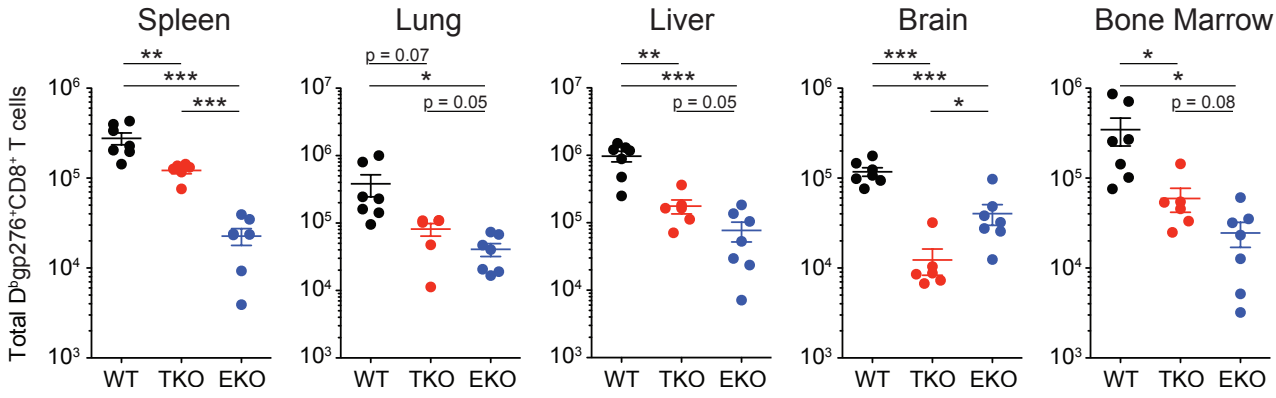
Spleen
Lung
Liver
Brain
Bone Marrow
Total Db gp276+CD8+ T cells
WT
TKO
EKO
p = 0.07
p = 0.05
p = 0.08

Figure S7

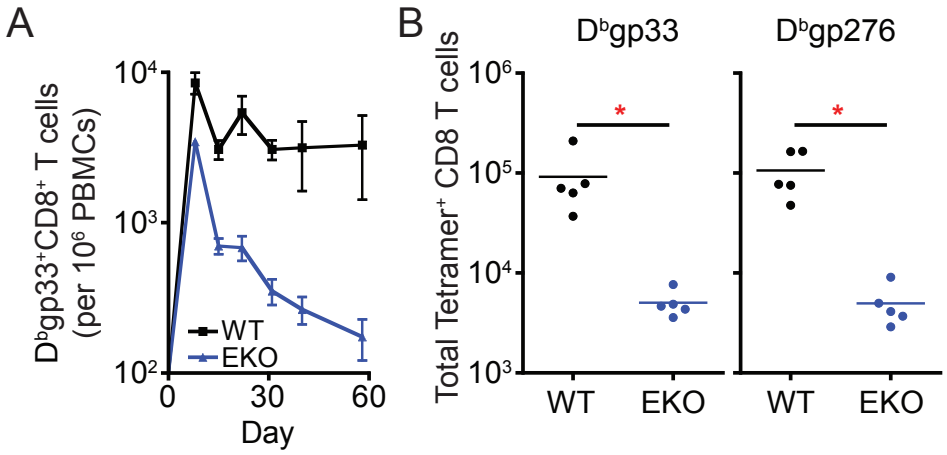
A
$D^bgp33^+CD8^+$ T cells (per 10^6 PBMCs)
10^4
10^3
10^2
WT
EKO
0
30
60
Day
B
D^bgp33
D^bgp276
Total $Tetramer^+$ CD8 T cells
10^6
10^5
10^4
10^3
*
*
WT
EKO
WT
EKO

Figure S8

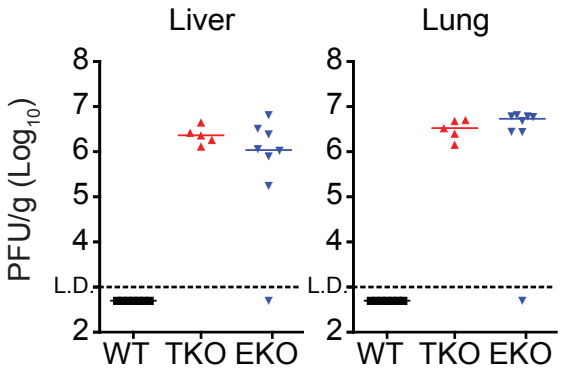

Figure S9

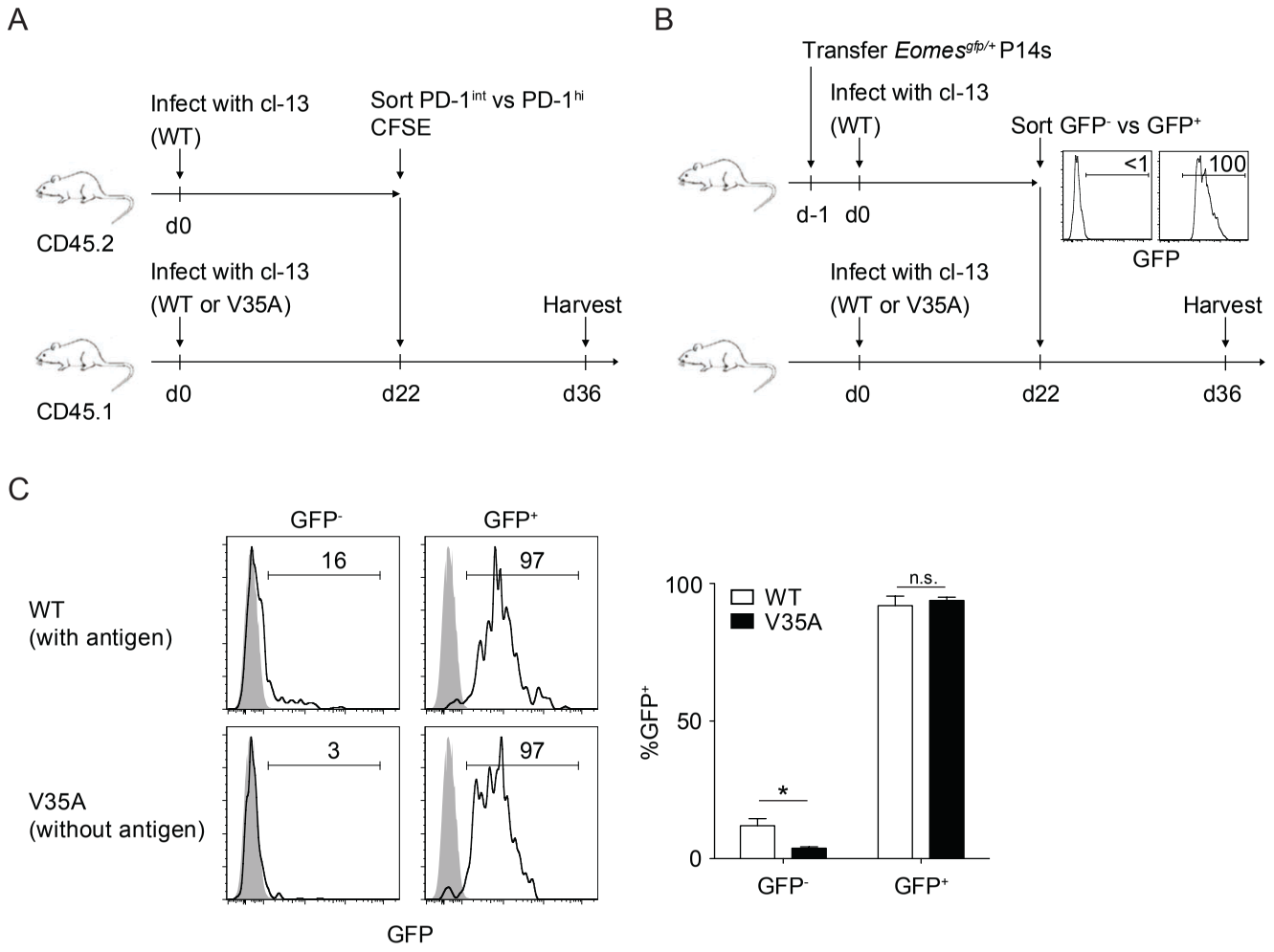
A
Infect with cl-13
(WT)
Sort PD-1int vs PD-1hi
CFSE
CD45.2
d0
Infect with cl-13
(WT or V35A)
Harvest
CD45.1
d0
d22
d36
B
Transfer Eomesgfp/+ P14s
Infect with cl-13
(WT)
Sort GFP- vs GFP+
<1
100
GFP
d-1
d0
Infect with cl-13
(WT or V35A)
Harvest
d0
d22
d36
C
GFP-
GFP+
16
97
WT
(with antigen)
3
97
V35A
(without antigen)
GFP
100
50
0
%GFP+
WT
V35A
n.s.
*
GFP-
GFP+

Figure S10

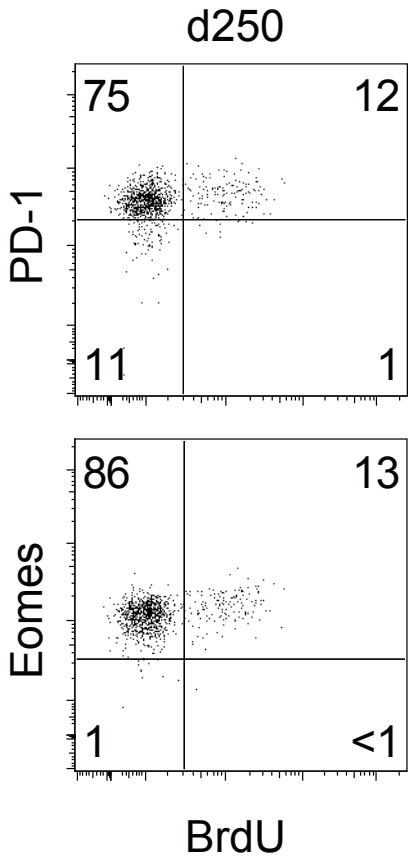

Figure S11

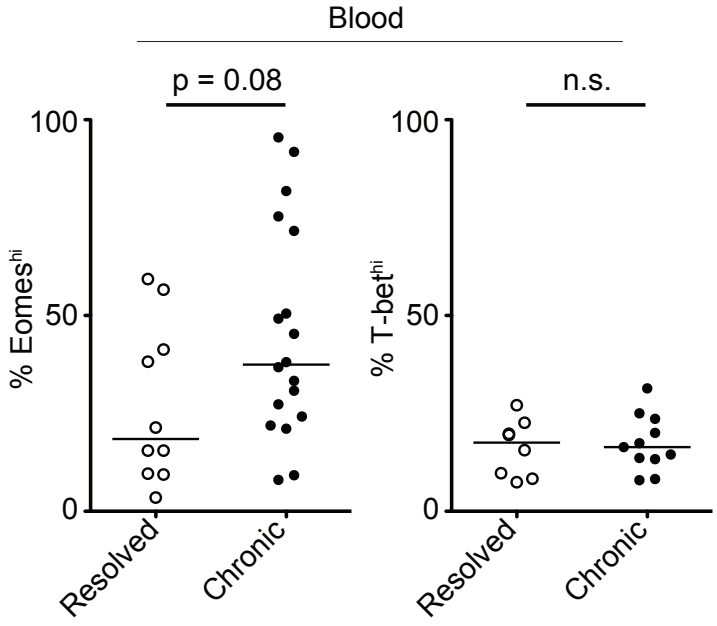
Blood
p = 0.08
n.s.
100
50
0
% Eomes^hi
% T-bet^hi
Resolved
Chronic
Resolved
Chronic

References

1. N. Sachsenberg *et al*., Turnover of $CD4^+$ and $CD8^+$ T lymphocytes in HIV-1 infection as measured by Ki-67 antigen. *J*. *Exp*. *Med*. **187**, 1295 (1998). doi:10.1084/jem.187.8.1295 Medline

2. M. Hellerstein *et al*., Directly measured kinetics of circulating T lymphocytes in normal and HIV-1-infected humans. *Nat*. *Med*. **5**, 83 (1999). doi:10.1038/4772 Medline

3. J. M. McCune *et al*., Factors influencing T-cell turnover in HIV-1-seropositive patients. *J*. *Clin*. *Invest*. **105**, R1 (2000). doi:10.1172/JCI8647 Medline

4. M. K. Hellerstein *et al*., Subpopulations of long-lived and short-lived T cells in advanced HIV-1 infection. *J*. *Clin*. *Invest*. **112**, 956 (2003). Medline

5. A. M. Intlekofer *et al*., Requirement for T-bet in the aberrant differentiation of unhelped memory $CD8^+$ T cells. *J*. *Exp*. *Med*. **204**, 2015 (2007). doi:10.1084/jem.20070841 Medline

6. N. S. Joshi *et al*., Inflammation directs memory precursor and short-lived effector $CD8^+$ T cell fates via the graded expression of T-bet transcription factor. *Immunity* **27**, 281 (2007). doi:10.1016/j.immuni.2007.07.010 Medline

7. A. M. Intlekofer *et al*., Anomalous type 17 response to viral infection by $CD8^+$ T cells lacking T-bet and eomesodermin. *Science* **321**, 408 (2008). doi:10.1126/science.1159806 Medline

8. A. Banerjee *et al*., Cutting edge: The transcription factor eomesodermin enables $CD8^+$ T cells to compete for the memory cell niche. *J*. *Immunol*. **185**, 4988 (2010). doi:10.4049/jimmunol.1002042

9. C. Kao *et al*., Transcription factor T-bet represses expression of the inhibitory receptor PD-1 and sustains virus-specific $CD8^+$ T cell responses during chronic infection. *Nat*. *Immunol*. **12**, 663 (2011). doi:10.1038/ni.2046 Medline

10. A. R. Hersperger *et al*., Increased HIV-specific $CD8^+$ T-cell cytotoxic potential in HIV elite controllers is associated with T-bet expression. *Blood* **117**, 3799 (2011). doi:10.1182/blood-2010-12-322727 Medline

11. P. Ribeiro-Dos-Santos *et al*., Chronic HIV infection affects the expression of the 2 transcription factors required for CD8 T-cell differentiation into cytolytic effectors. *Blood* **119**, 4928 (2012). doi:10.1182/blood-2011-12-395186

12. E. J. Wherry *et al*., Molecular signature of $CD8^+$ T cell exhaustion during chronic viral infection. *Immunity* **27**, 670 (2007). doi:10.1016/j.immuni.2007.09.006 Medline

13. H. Shin *et al*., A role for the transcriptional repressor Blimp-1 in $CD8^+$ T cell exhaustion during chronic viral infection. *Immunity* **31**, 309 (2009). doi:10.1016/j.immuni.2009.06.019 Medline

14. D. L. Barber *et al*., Restoring function in exhausted CD8 T cells during chronic viral infection. *Nature* **439**, 682 (2006). doi:10.1038/nature04444 Medline

15. C. L. Day *et al*., PD-1 expression on HIV-specific T cells is associated with T-cell exhaustion and disease progression. *Nature* **443**, 350 (2006). doi:10.1038/nature05115 Medline

16. S. D. Blackburn *et al*., Coregulation of $CD8^+$ T cell exhaustion by multiple inhibitory receptors during chronic viral infection. *Nat*. *Immunol*. **10**, 29 (2009). doi:10.1038/ni.1679 Medline

17. H. T. Jin *et al*., Cooperation of Tim-3 and PD-1 in CD8 T-cell exhaustion during chronic viral infection. *Proc*. *Natl*. *Acad*. *Sci*. *U*.*S*.*A*. **107**, 14733 (2010). doi:10.1073/pnas.1009731107 Medline

18. S. D. Blackburn *et al*., Tissue-specific differences in PD-1 and PD-L1 expression during chronic viral infection: Implications for CD8 T-cell exhaustion. *J*. *Virol*. **84**, 2078 (2010). doi:10.1128/JVI.01579-09 Medline

19. H. Shin, S. D. Blackburn, J. N. Blattman, E. J. Wherry, Viral antigen and extensive division maintain virus-specific CD8 T cells during chronic infection. *J*. *Exp*. *Med*. **204**, 941 (2007). doi:10.1084/jem.20061937 Medline

20. S. J. Arnold, J. Sugnaseelan, M. Groszer, S. Srinivas, E. J. Robertson, Generation and analysis of a mouse line harboring GFP in the Eomes/Tbr2 locus. *Genesis* **47**, 775 (2009). doi:10.1002/dvg.20562 Medline

21. M. Matloubian, R. J. Concepcion, R. Ahmed, $CD4^+$ T cells are required to sustain $CD8^+$ cytotoxic T-cell responses during chronic viral infection. *J. Virol.* **68**, 8056 (1994). Medline

22. J. M. Micallef, J. M. Kaldor, G. J. Dore, Spontaneous viral clearance following acute hepatitis C infection: A systematic review of longitudinal studies. *J. Viral Hepat.* **13**, 34 (2006). doi:10.1111/j.1365-2893.2005.00651.x Medline

23. F. Lechner *et al.*, $CD8^+$ T lymphocyte responses are induced during acute hepatitis C virus infection but are not sustained. *Eur. J. Immunol.* **30**, 2479 (2000). doi:10.1002/1521-4141(200009)30:9<2479::AID-IMMU2479>3.0.CO;2-B Medline

24. V. Kasprowicz *et al.*, High level of PD-1 expression on hepatitis C virus (HCV)-specific $CD8^+$ and $CD4^+$ T cells during acute HCV infection, irrespective of clinical outcome. *J. Virol.* **82**, 3154 (2008). doi:10.1128/JVI.02474-07 Medline

25. N. Nakamoto *et al.*, Functional restoration of HCV-specific CD8 T cells by PD-1 blockade is defined by PD-1 expression and compartmentalization. *Gastroenterology* **134**, 1927 (2008). doi:10.1053/j.gastro.2008.02.033 Medline

26. R. H. McMahan *et al.*, Tim-3 expression on $PD\text{-}1^+$ HCV-specific human CTLs is associated with viral persistence, and its blockade restores hepatocyte-directed in vitro cytotoxicity. *J. Clin. Invest.* **120**, 4546 (2010). doi:10.1172/JCI43127 Medline

27. M. L. Ciocca, B. E. Barnett, J. K. Burkhardt, J. T. Chang, S. L. Reiner, Cutting edge: Asymmetric memory T cell division in response to rechallenge. *J. Immunol.* **188**, 4145 (2012). doi:10.4049/jimmunol.1200176 Medline

28. E. J. Wherry *et al.*, Lineage relationship and protective immunity of memory CD8 T cell subsets. *Nat. Immunol.* **4**, 225 (2003). doi:10.1038/ni889 Medline

29. J. P. Casazza, M. R. Betts, L. J. Picker, R. A. Koup, Decay kinetics of human immunodeficiency virus-specific $CD8^+$ T cells in peripheral blood after initiation of highly active antiretroviral therapy. *J. Virol.* **75**, 6508 (2001). doi:10.1128/JVI.75.14.6508-6516.2001 Medline

30. E. J. Wherry, D. L. Barber, S. M. Kaech, J. N. Blattman, R. Ahmed, Antigen-independent memory CD8 T cells do not develop during chronic viral infection. *Proc. Natl. Acad. Sci. U.S.A.* **101**, 16004 (2004). doi:10.1073/pnas.0407192101 Medline

31. E. J. Wherry, T cell exhaustion. *Nat. Immunol.* **12**, 492 (2011). doi:10.1038/ni.2035 Medline

32. S. Finotto *et al.*, Development of spontaneous airway changes consistent with human asthma in mice lacking T-bet. *Science* **295**, 336 (2002). doi:10.1126/science.1065544 Medline

33. J. N. Blattman, E. J. Wherry, S. J. Ha, R. G. van der Most, R. Ahmed, Impact of epitope escape on PD-1 expression and CD8 T-cell exhaustion during chronic infection. *J. Virol.* **83**, 4386 (2009). doi:10.1128/JVI.02524-08 Medline

34. S. M. Gordon *et al.*, Requirements for eomesodermin and promyelocytic leukemia zinc finger in the development of innate-like $CD8^+$ T cells. *J. Immunol.* **186**, 4573 (2011). doi:10.4049/jimmunol.1100037 Medline

35. E. J. Wherry, J. N. Blattman, K. Murali-Krishna, R. van der Most, R. Ahmed, Viral persistence alters CD8 T-cell immunodominance and tissue distribution and results in distinct stages of functional impairment. *J. Virol.* **77**, 4911 (2003). doi:10.1128/JVI.77.8.4911-4927.2003 Medline

36. S. M. Gordon *et al.*, The transcription factors T-bet and Eomes control key checkpoints of natural killer cell maturation. *Immunity* **36**, 55 (2012). doi:10.1016/j.immuni.2011.11.016 Medline

37. B. M. Raabe, J. E. Artwohl, J. E. Purcell, J. Lovaglio, J. D. Fortman, Effects of weekly blood collection in C57BL/6 mice. *J. Am. Assoc. Lab. Anim. Sci.* **50**, 680 (2011). Medline

38. M. C. Cheung *et al.*, Body surface area prediction in normal, hypermuscular, and obese mice. *J. Surg. Res.* **153**, 326 (2009). doi:10.1016/j.jss.2008.05.002 Medline

39. R. Benner, F. Meima, G. M. van der Meulen, W. B. van Muiswinkel, Antibody formation in mouse bone marrow. I. Evidence for the development of plaque-forming cells in situ. *Immunology* **26**, 247 (1974). Medline

40. M. K. Slifka, M. Matloubian, R. Ahmed, Bone marrow is a major site of long-term antibody production after acute viral infection. *J. Virol.* **69**, 1895 (1995). Medline